Glyoxal photodissociation. An *ab initio* direct classical trajectory study of $C_2H_2O_2 \rightarrow H_2 + 2\,CO$

Xiaosong Li, John M. Millam, and H. Bernhard Schlegel[a)]
Department of Chemistry, Wayne State University, Detroit, Michigan 48202

(Received 14 November 2000; accepted 13 March 2001)

Unimolecular dissociation of glyoxal via a three-body fragmentation channel has been studied by direct classical trajectory calculations using Hartree–Fock (HF) and hybrid density functional methods (BH&HLYP, B3LYP) with split valence and polarized basis sets [HF/3-21G, BH&HLYP/6-311G(d,p) and B3LYP/6-311G(d,p)]. The transition state for $C_2H_2O_2 \rightarrow H_2 + 2$ CO has a dihedral angle of 90–110° between the carbonyl groups and a calculated barrier of ~59 kcal/mol above the *trans* conformer. To simulate the experimental conditions, trajectories were started from a microcanonical ensemble at the transition state with 4, 8, and 16 kcal/mol excess energy distributed among the vibrational modes and the transition vector. In agreement with experiment, the CO rotational distribution is very broad with a high $\langle J \rangle$. However, the calculations yielded more CO vibrational excitation for the triple dissociation channel than observed for all channels combined. Hydrogen is produced with low J but significant vibrational excitation, in accord with experiment. Similar to trajectory studies on $H_2CO \rightarrow H_2 + CO$, there is a good correlation between the energy released along the part of the reaction path where most of the H_2 bond length change occurs and the average vibrational excitation of the H_2 products. © *2001 American Institute of Physics.* [DOI: 10.1063/1.1369153]

INTRODUCTION

The photofragmentation of glyoxal, $C_2H_2O_2$, is an archetypal example of a three-body fragmentation and has captured the interest of both the experimental and theoretical communities (for leading references see Ref. 1) and is an important test for unimolecular reaction dynamics.[2] The absorption and emission spectra of singlet glyoxal are well understood[3–7] and the photophysics of the first excited state, S_1, has been studied extensively.[8–11] Intersystem crossing to the triplet is induced by collisions, and the triplet subsequently dissociates to formaldehyde and carbon monoxide.[12,13] Prior to 1980 this was thought to be the only pathway for photodissociation.[12,13] In the absence of collisions, no intersystem crossing occurs and S_1 is observed to have a lifetime of the order of 10^{-6} s.[8,14] Under collision free conditions, the fluorescence quantum yield is ~50% with the remainder returning to the ground state by nonradiative internal conversion.[15] In the early 1980's, Parmenter and co-workers provided strong evidence that glyoxal in S_1 dissociated in the absence of collisions and they observed H_2 as one of the major photolysis products.[16,17] The H_2 product could only come from a three-body fragmentation reaction, since there is not enough energy to produce H_2 by secondary fragmentation of formaldehyde. Hepburn *et al.*[18] unambiguously showed the presence of three distinct dissociation channels for collision-free photochemistry—triple dissociation forming $H_2 + 2$ CO (28%), $H_2CO + CO$ (65%), and a minor channel (7%) producing CO and an isomer of formaldehyde, possibly hydroxycarbene.

$$C_2H_2O_2 \rightarrow H_2 + 2\,CO, \tag{1}$$

$$\rightarrow H_2CO + CO, \tag{2}$$

$$\rightarrow HCOH + CO. \tag{3}$$

Typically, the zero-point level of S_1 or low-lying vibrational bands such as 8_0^1 are excited in the photodissociation experiments. Internal conversion yields a highly excited ground state with 63–65 kcal/mol excess energy. Burak *et al.*[14] ruled out the possibility of a long-lived intermediate, and determined that CO is formed almost entirely in $v=0$ but has a broad distribution of rotational states centered around $J=42$, with the angular momentum vector predominantly perpendicular to the recoil velocity vector. Dobeck *et al.*[1] observed H_2 in $v=1$ and $J=0-9$ with the angular momentum vector parallel to the recoil velocity vector. Analysis of shock tube experiments in the 1100–1540 K temperature range suggest that the activation energy for triple dissociation is ~47 kcal/mol,[19] and that the high-pressure limit for thermal unimolecular decomposition rate corresponds to an activation energy of 55 kcal/mol.[19]

Soon after the first experiments suggesting that glyoxal photodissociation occurred via a three-body fragmentation, theoretical calculations characterized the transition state for this reaction (whimsically termed the ''triple whammy'' reaction). Early work[20,21] indicated that the barrier for triple dissociation is low enough to permit this reaction under the experimental conditions, but that dissociation to $H_2CO + CO$ is 12–20 kcal/mol higher. Better calculations estimated the barrier for triple dissociation to be ~55 kcal/mol.[22] In a recent communication, we reported that more accurate calculations give a triple dissociation barrier of 59 kcal/mol.[23] The transition state for the $H_2CO + CO$ channel is found to be a

a)Electronic mail: hbs@chem.wayne.edu

1,2 hydrogen shift, markedly different than the earlier calculations. The calculated barrier of 55 kcal/mol for dissociation to H_2CO+CO is in good accord with the higher yield for this channel,[18] and is in excellent agreement with the activation energy obtained from the high-pressure limit for the thermal dissociation of glyoxal.[19] Recent calculations by Peslherbe *et al.* have confirmed these findings.[24]

In the present paper, we continue our study of the triple dissociation of glyoxal by using direct *ab initio* classical trajectory calculations to investigate the dynamics of the reaction. In this approach, trajectories are computed ''on the fly'' from electronic structure calculations, without first fitting a global analytical potential-energy surface (for a review see Ref. 25). Whenever energies, gradients or Hessians are needed for the trajectory integration, they are computed directly by molecular orbital methods. We have used a similar approach to study the dynamics of the photodissociation of formaldehyde, $H_2CO \rightarrow H_2+CO$.[26] In a subsequent paper, the same approach will be used to examine the H_2CO+CO channel of glyoxal photodissociation.

METHOD

The calculations were carried out with the development version of the GAUSSIAN series of programs.[27] Equilibrium geometries and transition states were optimized at the following levels of theories: Hartree-Fock [HF/3-21G, HF/6-311G(d,p)], second order Møller-Plesset perturbation theory [MP2/6-311G(d,p)], a modified version of Becke's half-and-half density functional method[28] [BH&HLYP/6-311G(d,p)], Becke's three parameter hybrid functional method[29] [B3LYP/6-311G(d,p)], and quadratic configuration interaction with single and double excitations[30] [QCISD/6-311G(d,p)]. The complete basis set extrapolation method of G. Peterson and co-workers[31] with the atomic pair natural orbital basis set (CBS-APNO) method was used to compute accurate heats of reaction and enthalpies of activation[31] (Table I). The mass-weighted steepest descent reaction paths were calculated using the method of Gonzalez and Schlegel.[32,33]

Ab initio classical trajectories were integrated using our Hessian based predictor-corrector method.[34] The Hessian was updated for five steps before being recalculated analytically.[35] A step size of 0.25 amu$^{1/2}$ bohr was used for all of the calculations, and the trajectories were stopped when the products were ~8 bohr apart or the gradient of the potential between product molecules was less than 1×10^{-5} hartree/bohr. The average time for a trajectory was 50–55 fs, and total energy was conserved to 10^{-7} hartree. Total angular momentum was conserved to better than $10^{-8}\,\hbar$ since projection methods were used to remove the overall angular forces.

The initial conditions for the trajectory calculations[36] were chosen to simulate the experimental photolysis of glyoxal from the zero point level of the S_1 state, which corresponds to 63 kcal/mol energy above the *trans* glyoxal ground state. Since there are a number of estimates of the barrier for unimolecular dissociation in the ground state, 47,[19] 55,[22] and 59 kcal/mol,[23] a range of initial energies was considered for the preliminary trajectory calculations at the HF/3-21G level—16, 8, and 4 kcal/mol excess energy above the zero-point level of the transition state. The trajectories were started at the transition state and the initial conditions were chosen to correspond to a microcanonical ensemble.[37] The total angular momentum was set to zero. For the motion along the reaction coordinate (i.e., along the transition vector), a uniform distribution of momentum in the direction of the products was used (none of these trajectories returned to reactants, suggesting that recrossing is not a significant problem for this system). For the microcanonical ensemble with 4 kcal/mol, eight samples were used with 0.0625, 0.25, 0.5625, 1.00, 1.5265, 2.25, 3.0625, 4.00 kcal/mol translational energy in the transition vector. The remaining energy was distributed quasi-classically among the vibrational modes perpendicular to the reaction path.[37] All vibrational states up to the maximum energy were generated within the harmonic oscillator approximation. For a given vibrational energy, E_{vib}, all states between E_{vib} and $E_{\mathrm{vib}}-\Delta E$ were selected; ΔE was adjusted to yield the desired number of states. For the 4 kcal/mol microcanonical ensemble with the

TABLE I. Reaction enthalpies and barrier heights for glyoxal.[a]

	$\Delta H^{\circ}_{r,298}$	$\Delta H^{\ddagger}_{298}$ forward
trans $C_2H_2O_2 \rightarrow$ cis $C_2H_2O_2$		
HF/3-21G	5.2	
HF/6-311G(d,p)	5.4	
MP2/6-311G(d,p)	3.9	
BH&HLYP/6-311G(d,p)	4.8	
B3LYP/6-311G(d,p)	4.3	
CBS-APNO	4.6	
experiment	3.9±0.6	
trans $C_2H_2O_2 \rightarrow H_2+CO+CO$		
HF/3-21G	−10.6	73.6
HF/6-311G(d,p)	−20.9	75.2
MP2/6-311G(d,p)	−10.9	54.9
BH&HLYP/6-311G(d,p)	−0.4	65.8
B3LYP/6-311G(d,p)	1.1	55.5
CBS-APNO	−1.8	59.2
experiment	−2.2±0.2	
trans $C_2H_2O_2 \rightarrow H_2CO+CO$		
HF/3-21G	−7.6	78.0
HF/6-311G(d,p)	−12.9	67.8
MP2/6-311G(d,p)	−5.3	56.6
BH&HLYP/6-311G(d,p)	−1.4	59.1
B3LYP/6-311G(d,p)	−0.2	51.6
CBS-APNO	−1.4	54.4
experiment	−1.8±0.2	
trans $C_2H_2O_2 \rightarrow$ HCOH+CO		
HF/3-21G	39.1	63.2
HF/6-311G(d,p)	34.9	69.5
MP2/6-311G(d,p)	50.5	59.3
BH&HLYP/6-311G(d,p)	50.1	62.6
B3LYP/6-311G(d,p)	52.8	56.5
CBS-APNO	51.2	59.7
trans $C_2H_2O_2 \rightarrow$ 2 HCO		
HF/3-21G	56.3	
HF/6-311G(d,p)	51.5	
MP2/6-311G(d,p)	68.5	
BH&HLYP/6-311G(d,p)	66.0	
B3LYP/6-311G(d,p)	65.2	
CBS-APNO	70.7	
experiment	71.5±0.2	

[a]Enthalpies at 298 K in kcal/mol; experimental data from Refs. 42–44.

TABLE II. Vibrational frequencies for glyoxal minima and transition states.[a]

	ν_1	ν_2	ν_3	ν_4	ν_5	ν_6	ν_7	ν_8	ν_9	ν_{10}	ν_{11}	ν_{12}
trans $C_2H_2O_2$												
HF/3-21G	311	356	601	948	1111	1218	1466	1494	1905	1937	3236	3239
MP2/6-311G(d,p)	149	333	563	836	1079	1098	1351	1398	1745	1759	3007	3012
BH&HLYP/6-311G(d,p)	151	384	584	863	1121	1132	1383	1430	1907	1923	3057	3060
B3LYP/6-311G(d,p)	143	332	552	818	1056	1076	1329	1376	1808	1810	2924	2929
cis $C_2H_2O_2$												
HF/3-21G	213	292	865	886	910	1241	1538	1542	1902	1932	3192	3227
MP2/6-311G(d,p)	144	283	764	826	862	1087	1406	1411	1741	1775	2951	1981
BH&HLYP/6-311G(d,p)	126	295	797	856	877	1141	1445	1454	1915	1940	2996	3029
B3LYP/6-311G(d,p)	133	281	741	813	824	1085	1388	1392	1800	1841	2859	2894
planar second-order saddle point for $C_2H_2O_2 \rightarrow H_2+CO+CO$												
MP2/6-311G(d,p)	1683i	153i	48	119	411	656	1065	1313	1327	1749	2037	2046
BH&HLYP/6-311G(d,p)	1806i	128i	113	139	366	657	1084	1321	1334	1756	2207	2218
B3LYP/6-311G(d,p)	1606i	136i	56	122	390	587	1048	1268	1283	1680	2092	2110
transition state for $C_2H_2O_2 \rightarrow H_2+CO+CO$												
HF/3-21G	2135i	194	202	306	350	749	1095	1432	1434	1768	2217	2219
MP2/6-311G(d,p)	1590i	123	209	224	628	742	967	1340	1418	1770	1995	2011
BH&HLYP/6-311G(d,p)	1850i	119	181	219	555	758	1022	1345	1422	1765	2165	2179
B3LYP/6-311G(d,p)	1649i	108	192	227	593	704	938	1297	1374	1706	2049	2062
transition state for $C_2H_2O_2 \rightarrow H_2CO+CO$												
HF/3-21G	1327i	233	509	667	856	1049	1360	1414	1526	1625	2229	3221
MP2/6-311G(d,p)	1097i	153	487	636	871	994	1164	1372	1548	1673	2068	3050
BH&HLYP/6-311G(d,p)	1088i	170	502	689	905	1046	1227	1409	1573	1754	2228	3062
B3LYP/6-311G(d,p)	1058i	182	493	637	883	968	1146	1350	1484	1627	2104	2993
transition state for $C_2H_2O_2 \rightarrow HCOH+CO$												
HF/3-21G	1691i	300	322	672	808	933	1344	1420	1596	2042	2221	3192
MP2/6-311G(d,p)	1282i	183	239	634	772	811	1301	1351	1531	1864	2055	3027
BH&HLYP/6-311G(d,p)	1512i	210	240	649	797	833	1312	1350	1632	1921	2198	3075
B3LYP/6-311G(d,p)	1273i	174	207	612	762	767	1273	1301	1530	1815	2098	2949

[a]Harmonic frequencies in cm^{-1} without scaling.

B3LYP/6-311G(d,p) electronic structure method, $\Delta E = 110\,cm^{-1}$ yielded 207 states (a detailed list of the initial states is available at http://www.chem.wayne.edu/Schlegel/supp-mat). For a specific vibrational mode with a given number of quanta, the initial phase is chosen randomly. Since the actual potential energy surface is not strictly harmonic, the initial vibrational coordinates and momenta generated by this procedure are scaled to yield the desired vibrational energy.[37] Approximately 100 trajectories were integrated at the HF/3-21G and BH&HLYP/6-311G(d,p) levels of theory for each energy, and 207 trajectories were integrated at the B3LYP/6-311G(d,p) level for 4 kcal/mol excess energy. Product energy distributions were analyzed according to Ref. 36. Where appropriate, error bars of one standard deviation are included in the plots.

RESULTS AND DISCUSSION

Structures and energetics

Experimentally, the ground state (S_0) of glyoxal is planar and in a *trans* conformation; the *cis* conformer is 3.9 ± 0.6 kcal/mol higher and is separated from the *trans* conformer by a barrier of $\sim$1.3 kcal/mol.[38,39] The present calculations agree well with the experimental geometries[38,39] and place the *cis* conformer 4.6 kcal/mol higher than the *trans* conformer at the CBS-APNO level of theory (Table I). Other theoretical studies also yield an energy difference 1 to 2 kcal/mol higher than experiment.[20,24,40] The calculated vibrational frequencies are listed in Table II. These are in good agreement with the available experimental data[41] and with other calculations.[40] In the first excited singlet (S_1), the calculated *cis-trans* energy difference is very small, but the barrier for

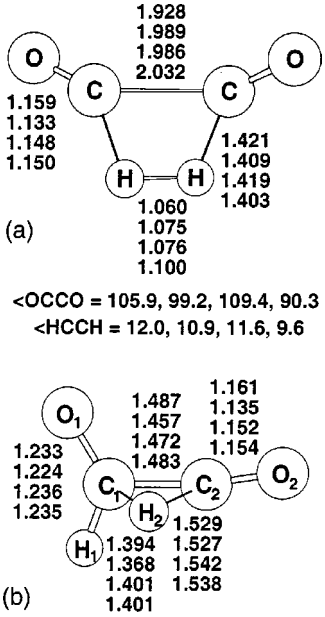

FIG. 1. Optimized geometries of the transition states for (a) glyoxal $\rightarrow H_2+2\,CO$ and (b) glyoxal$\rightarrow H_2CO+CO$ [from top to bottom: MP2, BH&HLYP, B3LYP, and QCISD with the 6-311G(d,p) basis].

TABLE III. Optimized geometries for glyoxal minima and transition states.[a]

	CC	C_1O_1	C_2O_2	C_1H_1	C_2H_2	HH	CCO_1	CCO_2	CCH_1	CCH_2	OCCO	HCCH
trans $C_2H_2O_2$												
HF/3-21G	1.504	1.206	···	1.082	···	3.100	121.4	···	114.3	···	0.0	0.0
MP2/6-311G(*d*,*p*)	1.522	1.213	···	1.107	···	3.166	121.6	···	114.6	···	0.0	0.0
BH&HLYP/6-311G(*d*,*p*)	1.515	1.189	···	1.098	···	3.147	121.4	···	114.7	···	0.0	0.0
B3LYP/6-311G(*d*,*p*)	1.528	1.202	···	1.109	···	3.171	121.6	···	114.4	···	0.0	0.0
QCISD/6-311G(*d*,*p*)	1.530	1.206	···	1.108	···	3.173	121.5	···	114.6	···	0.0	0.0
cis $C_2H_2O_2$												
HF/3-21G	1.509	1.205	···	1.083	···	2.389	123.1	···	114.0	···	0.0	0.0
MP2/6-311G(*d*,*p*)	1.537	1.210	···	1.110	···	2.483	122.2	···	115.2	···	0.0	0.0
BH&HLYP/6-311G(*d*,*p*)	1.531	1.185	···	1.101	···	2.473	122.2	···	115.3	···	0.0	0.0
B3LYP/6-311G(*d*,*p*)	1.545	1.198	···	1.113	···	2.478	122.5	···	114.8	···	0.0	0.0
QCISD/6-311G(*d*,*p*)	1.544	1.203	···	1.111	···	2.488	122.2	···	115.1	···	0.0	0.0
planar second-order saddle point for $C_2H_2O_2 \rightarrow H_2+CO+CO$												
MP2/6-311G(*d*,*p*)	2.137	1.155	···	1.422	···	1.062	153.7	···	67.8	···	0.0	0.0
BH&HLYP/6-311G(*d*,*p*)	2.156	1.130	···	1.407	···	1.076	154.6	···	67.4	···	0.0	0.0
B3LYP/6-311G(*d*,*p*)	2.233	1.144	···	1.408	···	1.081	158.2	···	65.9	···	0.0	0.0
QCISD/6-311G(*d*,*p*)	2.143	1.149	···	1.404	···	1.099	154.0	···	68.2	···	0.0	0.0
transition state for $C_2H_2O_2 \rightarrow H_2+CO+CO$												
HF/3-21G	2.067	1.144	···	1.410	···	1.096	149.8	···	69.9	···	0.0	0.0
MP2/6-311G(*d*,*p*)	1.928	1.159	···	1.421	···	1.060	138.1	···	71.4	···	105.9	12.0
BH&HLYP/6-311G(*d*,*p*)	1.989	1.133	···	1.409	···	1.075	141.1	···	70.4	···	99.2	10.9
B3LYP/6-311G(*d*,*p*)	1.986	1.148	···	1.419	···	1.076	139.0	···	70.5	···	109.4	11.6
QCISD/6-311G(*d*,*p*)	2.032	1.150	···	1.403	···	1.100	143.8	···	70.1	···	90.3	9.6
transition state for $C_2H_2O_2 \rightarrow H_2CO+CO$												
HF/3-21G	1.485	1.240	1.142	1.082	1.621	1.863	124.4	179.1	106.2	55.0	−104.2	87.7
MP4/6-311G(*d*,*p*)	1.487	1.233	1.161	1.101	1.529	1.855	120.9	170.4	109.4	55.1	−20.8	86.4
BH&HLYP/6-311G(*d*,*p*)	1.457	1.224	1.135	1.095	1.527	1.843	122.3	175.3	108.8	54.5	−42.4	88.3
B3LYP/6-311G(*d*,*p*)	1.472	1.236	1.152	1.100	1.542	1.870	118.7	167.4	111.8	55.3	−17.2	86.4
QCISD/6-311G(*d*,*p*)	1.483	1.235	1.154	1.101	1.538	1.869	120.8	171.1	109.7	55.2	−24.3	87.1
transition state for $C_2H_2O_2 \rightarrow HCOH+CO$												
HF/3-21G	2.031	1.249	1.145	1.086	1.367	2.870	85.3	133.2	157.8	61.1	180.0	180.0
MP2/6-311G(*d*,*p*)	2.090	1.252	1.154	1.104	1.417	2.812	84.3	136.2	164.1	57.1	180.0	180.0
BH&HLYP/6-311G(*d*,*p*)	2.048	1.228	1.132	1.095	1.390	2.822	85.3	135.1	160.6	58.7	180.0	180.0
B3LYP/6-311G(*d*,*p*)	2.122	1.243	1.144	1.106	1.421	2.845	84.0	137.1	163.2	57.1	179.9	179.9
QCISD/6-311G(*d*,*p*)	2.057	1.248	1.149	1.105	1.387	2.836	85.3	135.9	161.6	58.8	180.0	180.0

[a]Bond lengths in Å, angles in degrees; see Fig. 1 for atom numbering.

internal rotation may be higher than in S_0, judging from torsional frequencies.[40]

As we reported previously, the glyoxal reaction enthalpies computed at the CBS-APNO level (Table I) are in very good agreement with the available experimental data.[42–44] The B3LYP and BH&HLYP energetics are also in good agreement, but the HF calculations have errors that are 10–20 kcal/mol larger. Similar trends in the quality of the calculated energetics were obtained for $H_2CO \rightarrow H_2+CO$.[26]

The optimized transition structures are presented in Fig. 1 and Table III. The structure for glyoxal$\rightarrow H_2+2$ CO [Fig. 1(a)] agrees well with earlier coupled cluster calculations with a polarized double zeta basis (CCSD/DZP) when the system is constrained to be planar.[22] However, except for HF/3-21G, all levels of theory considered in the present work show that the planar structure is a second order saddle point. Full optimization at MP2, BH&HLYP, B3LYP, and QCISD leads to a transition state with a dihedral angle of 90°–110° between the carbonyl groups [Fig. 1(a)]. Because the potential-energy surface is very flat, the twisted transition state is only 1 kcal/mol lower than the planar second-order saddle point. Reaction path following was used to confirm that this transition state connects glyoxal and H_2+2 CO at MP2 and B3LYP. At the CBS-APNO and G3 levels of theory, the calculated barrier height for glyoxal$\rightarrow H_2+CO+CO$[23,24] is ~5 kcal/mol higher than the extrapolated value of Scuseria *et al.*[22] As a point of calibration, it should be noted that the CBS-APNO and G3 calculations for the $H_2CO \rightarrow H_2+CO$ barrier are in excellent agreement with experiment[45] and higher level theoretical calculations.[46]

The transition structure for glyoxal$\rightarrow H_2CO+CO$ is quite different than described in early work.[21] As we[23] and Peslherbe[24] have reported recently, the correct structure [Fig. 1(b)] is a 1,2 hydrogen shift across the C–C bond. The HCO group rotates to accept the shifting hydrogen and become the formaldehyde product. The C–H distances for the migrating hydrogen are typical for 1,2 hydrogen shifts,[47] and the C–C bond is still intact, similar to other 1,2 hydrogen shifts. Reaction path following confirms that this transition structure connects glyoxal and H_2CO+CO. This transition state is ~5 kcal/mol lower than the triple dissociation transition state, in accord with the observed higher yield for the H_2CO+CO channel than for the triple dissociation channel. The barrier heights of 54.6 and 55.4 kcal/mol calculated at the CBS-APNO and G3 levels,[23,24] respectively, are in excellent agreement with the experimental activation energy of 55.1

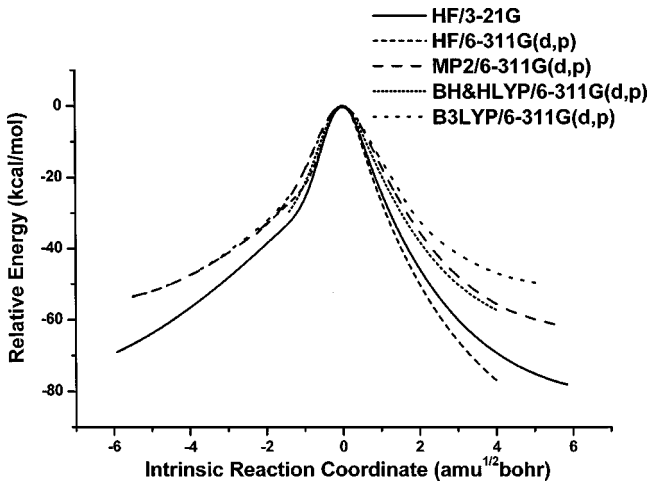

FIG. 2. Potential energy along the reaction path for glyoxal→H_2+2 CO at HF/3-21G, HF/6-311G(d,p), MP2/6-311G(d,p), BH&HLYP/6-311G(d,p), and B3LYP/6-311G(d,p).

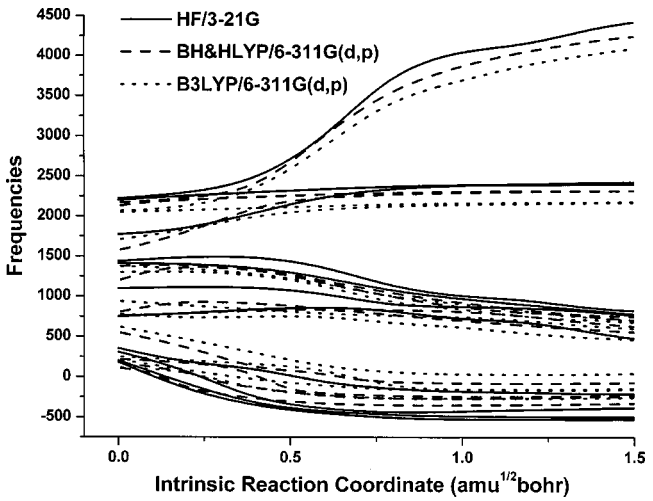

FIG. 3. Vibrational frequencies along the reaction path at HF/3-21G, BH&HLYP/6-311G(d,p), and B3LYP/6-311G(d,p).

kcal/mol obtained from high pressure limit.[19] The structure reported in earlier work[21] appears to be on the glyoxal→2 HCO pathway and is ~12 kcal/mol higher than the triple dissociation transition state. Energetics calculated at the CBS-APNO level support this interpretation.[23]

The frequently quoted experimental activation energy of 47 kcal/mol[19] for triple dissociation of glyoxal was based on a fit of a reaction mechanism. It assumed that the activation energy for glyoxal→H_2CO+CO was 10 kcal/mol higher than for the triple dissociation channel, based on earlier calculations[21] now shown to be incorrect.[23,24] The calculations described above place the triple dissociation channel 5 kcal/mol higher than the formaldehyde channel. The fact that these calculations agree very well with the activation energies for H_2CO→H_2+CO and glyoxal→H_2CO+CO, suggests that the 59–61 kcal/mol barrier calculated for the triple dissociation channel should also be reliable.

Reaction path

Figure 2 shows the potential-energy profile along the mass-weighted steepest descent reaction path (intrinsic reaction coordinate). The potential-energy released at the HF/3-21G and HF/6-311G(d,p) levels is 20–30 kcal/mol too large, but the MP2/6-311G(d,p), BH&HLYP/6-311G(d,p) and B3LYP/6-311G(d,p) results are within ±6 kcal/mol of the CBS-APNO value. Similar to formaldehyde,[26] most of the geometry changes in the H_2 and CO bond lengths are finished by $s=1$ amu$^{1/2}$ bohr [this corresponds to C–C and C–H bond lengths of 2.058 and 1.751 Å at B3LYP/6-311G(d,p) level]. Only 27%–34% of energy has been released by this point, compared to 50% for formaldehyde.[26] This is understandable, since there is more van der Waals repulsion between the three fragments in the glyoxal reaction than between the two fragments in formaldehyde. The vibrational frequencies along path are compared in Fig. 3. The behavior is similar at the three levels considered.

Dynamics

The vibrational populations of the H_2 and CO products of the triple dissociation are shown in Fig. 4 for different amounts of excess energy at same level of theory. Trajecto-

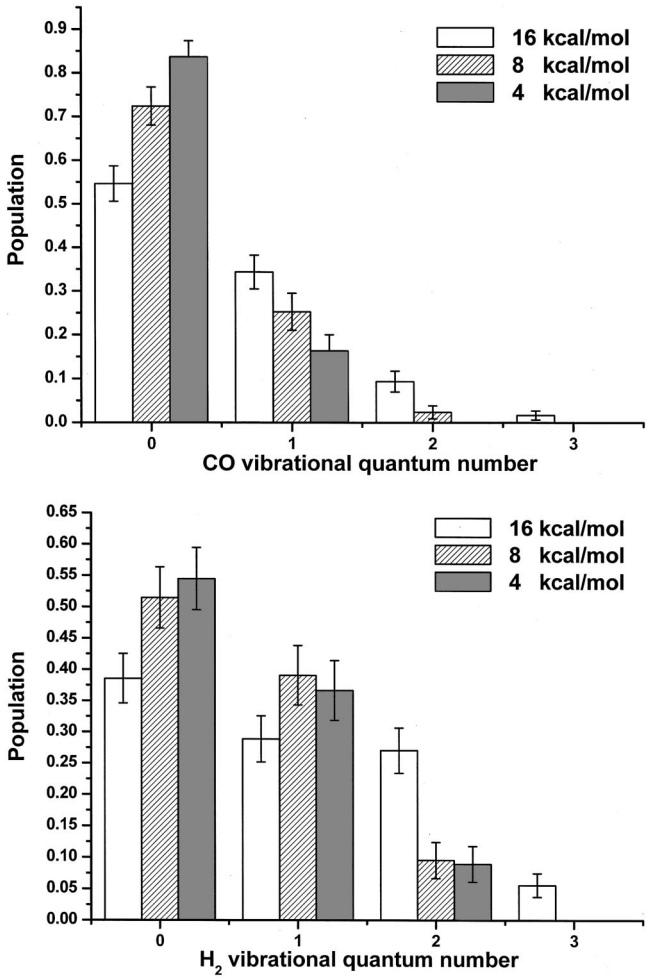

FIG. 4. Vibrational populations for CO and H_2 computed at HF/3-21G for microcanonical ensembles with 16, 8, and 4 kcal/mol excess energy above the transition state.

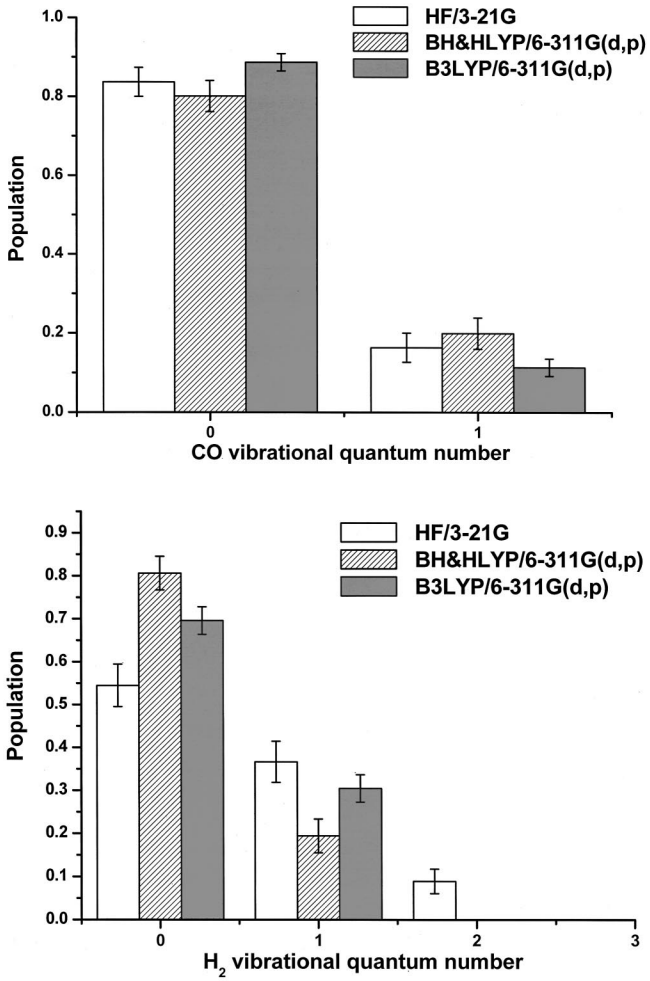

FIG. 5. Vibrational populations for CO and H_2 computed at HF/3-21G, BH&HLYP/6-311G(d,p), and B3LYP/6-311G(d,p) for a microcanonical ensemble with 4 kcal/mol excess energy.

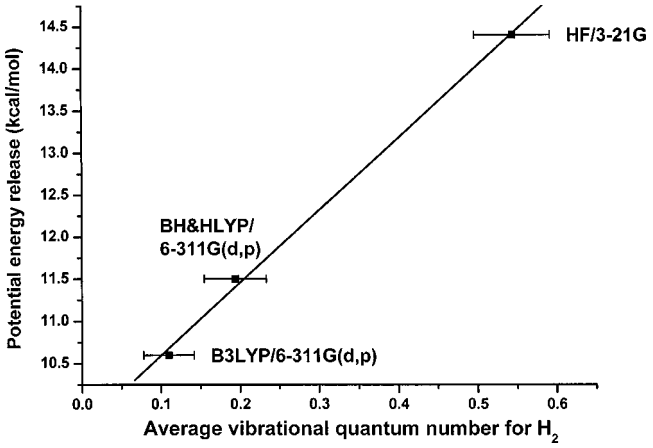

FIG. 6. Average vibrational quantum numbers for CO and H_2 vs energy release for HF/3-21G, BH&HLYP/6-311G(d,p), and B3LYP/6-311G(d,p) for a microcanonical ensemble with 4 kcal/mol excess energy.

ries were calculated at the HF/3-21G level with a total of 16, 8, and 4 kcal/mol energy above the transition state, distributed in a microcanonical ensemble among translation along the reaction coordinate and vibration perpendicular to the reaction coordinate. For the same energy, the H_2 shows a higher degree of vibrational excitation than CO. As might be anticipated, the vibrational excitation for both H_2 and CO decreases with decreasing amounts of excess energy. The fact that little or no vibrationally excited CO is observed experimentally implies that the excess energy is small, which in turn supports the higher calculated barrier for triple dissociation (59 kcal/mol). A microcanonial ensemble of 4 kcal/mol excess energy above the transition state is used for all further calculations in the present study.

With 4 kcal/mol excess energy, the average translational energy for H_2 is 43.4, 34.7, and 27.5 kcal/mol for the HF/3-21G, BH&HLYP/6-311G(d,p), and B3LYP/6-311G(d,p) levels of theory, respectively, compared to the experimental value of 31 kcal/mol.[1] For $v=1$, the average translational energy of H_2 is 3–6 kcal/mol lower than for $v=0$. The average translational energy for CO is 11.6, 7.6, and 7.4 kcal/mol for the HF/3-21G, BH&HLYP/6-311G(d,p), and B3LYP/6-311G(d,p) levels of theory, respectively, compared to the experimental value of 15 kcal/mol[18] (note that, experimentally, more than half of the CO comes from the H_2CO+CO channel and the average CO translational energy for this channel is expected to be higher). There appears to be no correlation between the translational energy of the two CO's produced in the triple dissociation reaction.

Figure 5 compares the vibrational populations of H_2 and CO obtained from trajectories computed at different levels of theory but with the same energy [HF/3-21G, BH&HLYP/6-311G(d,p), and B3LYP/6-311G(d,p) for the 4 kcal/mol microcanonical ensemble]. The calculations show much less vibrational excitation of H_2 than formaldehyde, despite the fact that the H_2 distance in the transition state is similar. Experimentally, the $v=1$ population for H_2 is estimated to be greater than 0.15 (the $v=0$ population cannot be observed for technical reasons[1]). All three levels of theory are in agreement with this. For CO, the B3LYP calculations show a population of 0.11 in $v=1$. None of the trajectories produced $v=1$ in both CO's. Experiments indicate the population of $v=1$ in the product CO is less than 0.05. Because the H_2CO+CO channel has a higher branching ratio, less than half of the CO product comes from the triple dissociation reaction. Preliminary results indicate that the CO from the H_2CO+CO channel is produced with almost no vibrational excitation; thus the combined distribution should be in better accord with the experimental findings.

For $H_2CO \rightarrow H_2+CO$, we found a good correlation between the average vibrational excitation of the H_2 product and the energy released while most of the geometric changes were occurring.[26] Figure 6 indicates that a similar relation is found for glyoxal triple dissociation. At the position along the reaction path where the changes in the H_2 bond are 80% complete, the potential energy release is 14.3, 11.5, and 10.6 kcal/mol for the HF/3-21G, BH&HLYP/6-311G(d,p), and B3LYP/6-311G(d,p) levels of theory, respectively. Compared to formaldehyde photodissociation, there is less vibrational excitation since less energy is released during part of the path in which the H_2 bond formed.

The rotational state populations of the H_2 and CO products are presented in Fig. 7. The calculations show that the

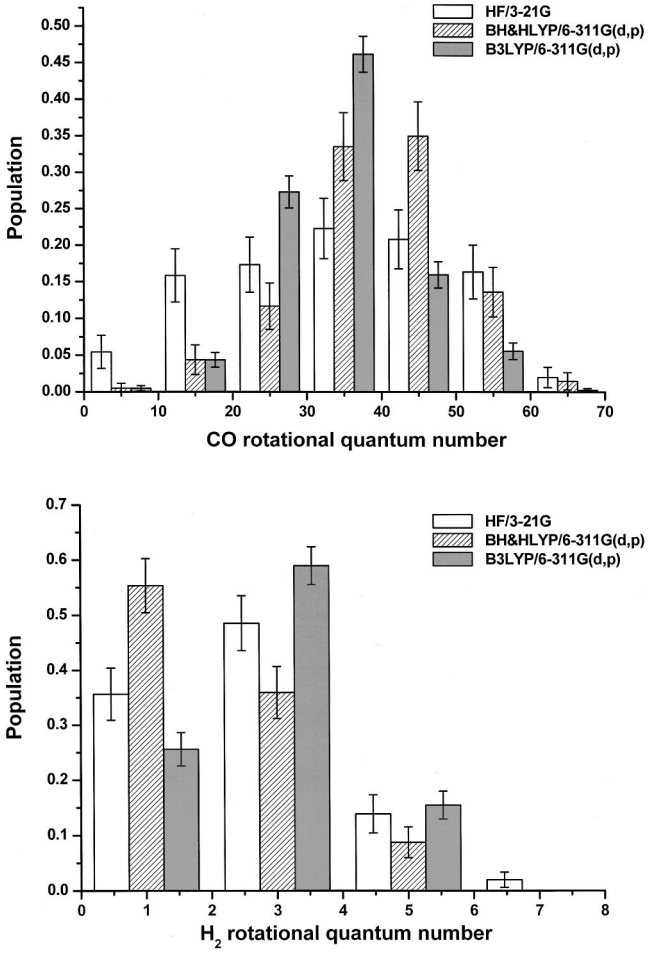

FIG. 7. Rotational populations for CO and H_2 at HF/3-21G, BH&HLYP/6-311G(d,p), and B3LYP/6-311G(d,p) for a microcanonical ensemble with 4 kcal/mol excess energy.

distributions for CO are very wide, ranging up to $J=0$ to 70, with average values of 34.4, 39.4, and 34.0 for the HF/3-21G, BH&HLYP/6-311G(d,p), and B3LYP/6-311G(d,p) levels of theory, respectively. Experiment also shows a similarly broad distribution with a maximum near $J=42$. This had been interpreted as arising primarily from the H_2CO+CO channel,[14] but the present calculations indicate that the triple dissociation path also has a broad distribution with a high $\langle J\rangle$. The H_2 product is calculated to be in low rotational states, $J=0-9$, with $\langle J\rangle=3$, in agreement with the observed distribution. For both H_2 and CO, there is no appreciable dependence of $\langle J\rangle$ on the vibrational excitation. There appears to be no rotational correlation between two CO's in a reaction.

CONCLUSION

Direct classical trajectories for glyoxal three-body dissociation channel calculated at the HF, BH&HLYP, and B3LYP levels of theory lead to vibrational and rotational distributions in good agreement with experiment for H_2. The calculated rotational distribution for CO compares very well with experiment, but the computations yield more vibrational excitation for the triple dissociation channel than observed for all channels combined. There is a useful relation between the average vibrational excitation of the H_2 product and the energy released at 80% of the H_2 bond completion. Comparable direct classical trajectory calculations are in progress for the glyoxal $\rightarrow H_2CO+CO$ channel.

ACKNOWLEDGMENTS

This work was supported by a grant from the National Science Foundation (Grant Nos. CHE 9874005 and CISE 9977815). The authors would like to thank William L. Hase for helpful discussions and Wayne State University for computer time.

[1] L. M. Dobeck, H. M. Lambert, W. Kong, P. J. Pisano, and P. L. Houston, J. Phys. Chem. A **103**, 10312 (1999).
[2] T. Baer and W. L. Hase, *Unimolecular Reaction Dynamics* (Oxford University Press, New York, 1996).
[3] J. Paldus and D. A. Ramsay, Can. J. Phys. **45**, 1389 (1967).
[4] F. W. Birss, D. B. Braund, A. R. H. Cole *et al.*, Can. J. Phys. **55**, 390 (1977).
[5] G. H. Atkinson, R. A. Malstrom, and M. E. McIlwain, J. Mol. Spectrosc. **76**, 164 (1979).
[6] G. H. Atkinson, R. A. Malstrom, and M. E. McIlwain, J. Mol. Spectrosc. **76**, 182 (1979).
[7] C. Cossart-Magos, A. Frad, and A. Tramer, Spectrochim. Acta Part A **34**, 195 (1978).
[8] R. A. Beyer, P. F. Zittel, and W. C. Lineberger, J. Chem. Phys. **62**, 4016 (1975).
[9] R. A. Beyer and W. C. Lineberger, J. Chem. Phys. **62**, 4024 (1975).
[10] P. F. Zittel and W. C. Lineberger, J. Chem. Phys. **66**, 2972 (1977).
[11] C. Michel and A. Tramer, Chem. Phys. **42**, 315 (1979).
[12] R. Naaman, D. M. Lubman, and R. N. Zare, J. Chem. Phys. **71**, 4192 (1979).
[13] G. H. Atkinson, M. E. McIlwain, and C. G. Venkatesh, J. Chem. Phys. **68**, 726 (1978).
[14] I. Burak, J. W. Hepburn, N. Sivakumar, G. E. Hall, G. Chawla, and P. L. Houston, J. Chem. Phys. **86**, 1258 (1987).
[15] B. G. MacDonald and E. K. C. Lee, J. Chem. Phys. **71**, 5049 (1979).
[16] G. W. Loge, C. S. Parmenter, and B. F. Rordorf, Chem. Phys. Lett. **74**, 309 (1980).
[17] G. W. Loge and C. S. Parmenter, J. Phys. Chem. **85**, 1653 (1981).
[18] J. W. Hepburn, R. J. Buss, L. J. Butler, and Y. T. Lee, J. Phys. Chem. **87**, 3638 (1983).
[19] K. Saito, T. Kakumoto, and I. Murakami, J. Phys. Chem. **88**, 1182 (1984).
[20] Y. Osamura and H. F. Schaefer, J. Chem. Phys. **74**, 4576 (1981).
[21] Y. Osamura, H. F. Schaefer, M. Dupuis, and W. A. Lester, J. Chem. Phys. **75**, 5828 (1981).
[22] G. E. Scuseria and H. F. Schaefer, J. Am. Chem. Soc. **111**, 7761 (1989).
[23] X. S. Li and H. B. Schlegel, J. Chem. Phys. **114**, 8 (2001).
[24] D. M. Koch, N. N. Khieu, and G. H. Peslherbe, J. Phys. Chem. A 105 (2001).
[25] K. Bolton, W. L. Hase, and G. H. Peslherbe, in *Modern Methods for Multidimensional Dynamics Computation in Chemistry*, edited by D. L. Thompson (World Scientific, Singapore, 1998).
[26] X. Li, J. M. Millam, and H. B. Schlegel, J. Chem. Phys. **113**, 10062 (2000).
[27] M. J. Frisch, G. W. Trucks, H. B. Schlegel *et al.*, GAUSSIAN, Gaussian, Inc., Pittsburgh, PA.
[28] A. D. Becke, J. Chem. Phys. **98**, 1372 (1993).
[29] A. D. Becke, J. Chem. Phys. **98**, 5648 (1993).
[30] J. A. Pople, M. Head-Gordon, and K. Raghavachari, J. Chem. Phys. **87**, 5968 (1987).
[31] J. A. Montgomery, J. W. Ochterski, and G. A. Petersson, J. Chem. Phys. **101**, 5900 (1994).
[32] C. Gonzalez and H. B. Schlegel, J. Chem. Phys. **90**, 2154 (1989).
[33] C. Gonzalez and H. B. Schlegel, J. Phys. Chem. **94**, 5523 (1990).
[34] J. M. Millam, V. Bakken, W. Chen, W. L. Hase, and H. B. Schlegel, J. Chem. Phys. **111**, 3800 (1999).
[35] V. Bakken, J. M. Millam, and H. B. Schlegel, J. Chem. Phys. **111**, 8773 (1999).

[36] W. L. Hase, in *Encyclopedia of Computational Chemistry*, edited by P. v. R. Schleyer, N. L. Allinger, T. Clark, J. Gasteiger, P. A. Kollman, H. F. Schaefer III, and P. R. Schreiner (Wiley, New York, 1998).
[37] G. H. Peslherbe, H. Wang, and W. L. Hase, in *Monte Carlo Methods in Chemical Physics, Vol. 105*, edited by D. M. Ferguson, J. I. Siepmann, and D. G. Truhlar (Wiley, New York, 1999).
[38] G. N. Currie and D. A. Ramsay, Can. J. Phys. **49**, 317 (1971).
[39] J. R. Durig, C. C. Tong, and Y. S. Li, J. Chem. Phys. **57**, 4425 (1972).
[40] J. F. Stanton and J. Gauss, Spectrochim. Acta, Part A **53**, 1153 (1997).
[41] R. Y. Dong, R. Nanes, and D. A. Ramsay, Can. J. Chem. **71**, 1595 (1993).
[42] M. W. Chase, Jr., J. Phys. Chem. Ref. Data Monogr. **9**, 1 (1998).
[43] R. A. Fletcher and G. Pilcher, Trans. Faraday Soc. **66**, 794 (1970).
[44] D. L. Baulch, R. A. Cox, P. J. Crutzen, R. F. Hampson, J. A. Kerr, J. Troe, and R. T. Watson, J. Phys. Chem. Ref. Data **11**, 327 (1982).
[45] W. F. Polik, D. R. Guyer, and C. B. Moore, J. Chem. Phys. **92**, 3453 (1990).
[46] D. Feller, M. Dupuis, and B. C. Garrett, J. Chem. Phys. **113**, 218 (2000).
[47] J. A. Pople, K. Raghavachari, M. J. Frisch, J. S. Binkley, and P. v. R. Schleyer, J. Am. Chem. Soc. **105**, 6389 (1983).